

## Article

# Production and Characterization of Polyhydroxyalkanoates from Wastewater via Mixed Microbial Cultures and Microalgae

Simone Bagatella <sup>1,\*</sup> , Riccardo Ciapponi <sup>1</sup> , Elena Ficara <sup>2</sup>, Nicola Frison <sup>3</sup> and Stefano Turri <sup>1</sup>

<sup>1</sup> Dipartimento di Chimica, Materiali e Ingegneria Chimica “Giulio Natta”, Politecnico di Milano, Piazza Leonardo da Vinci 32, 20133 Milan, Italy; riccardo.ciapponi@polimi.it (R.C.); stefano.turri@polimi.it (S.T.)

<sup>2</sup> Dipartimento di Ingegneria Civile e Ambientale, Politecnico di Milano, Piazza Leonardo da Vinci 32, 20133 Milan, Italy; elena.ficara@polimi.it

<sup>3</sup> Dipartimento di Biotecnologie, Università degli Studi di Verona, Via S. Francesco 22, 37129 Verona, Italy; nicola.frison@univr.it

\* Correspondence: simone.bagatella@polimi.it

**Abstract:** In the context of circular economy and sustainable production of materials, this project investigated the feasibility of producing sustainable polyhydroxyalkanoates (PHA) from microalgae and sludge used in the treatment of municipal wastewater. The overall process was studied looking at the main steps: microalgae production, fermentation of the biomass, production and characterization of the PHAs. It was possible to obtain blends of hydroxybutyrate-hydroxyvalerate copolymers with high molecular weights and different compositions depending on the nature of the feedstock (mixed volatile fatty acids). In some cases, almost completely amorphous PHA materials were obtained, suggesting a potential diversification of uses and applications.

**Keywords:** microalgae; wastewater; fermentation; polyhydroxyalkanoates; characterization



**Citation:** Bagatella, S.; Ciapponi, R.; Ficara, E.; Frison, N.; Turri, S. Production and Characterization of Polyhydroxyalkanoates from Wastewater via Mixed Microbial Cultures and Microalgae. *Sustainability* **2022**, *14*, 3704. <https://doi.org/10.3390/su14063704>

Academic Editors: Matia Mainardis, Arianna Catenacci and Fabiano Asunis

Received: 3 February 2022

Accepted: 18 March 2022

Published: 21 March 2022

**Publisher’s Note:** MDPI stays neutral with regard to jurisdictional claims in published maps and institutional affiliations.



**Copyright:** © 2022 by the authors. Licensee MDPI, Basel, Switzerland. This article is an open access article distributed under the terms and conditions of the Creative Commons Attribution (CC BY) license (<https://creativecommons.org/licenses/by/4.0/>).

## 1. Introduction

Polymers are important materials in the global economy, and modern daily life is unthinkable without them. They are widely used in packaging films, plastics, structural composites, textiles, protective coatings and adhesives. All technological indicators show a progressively increasing use of polymers in a variety of applications, where they can effectively replace, for example, metals saving weight and cost. At the same time, however, the management of end-of-life (EoL) plastics is still problematic for its impact on the environment. Action on plastics was already identified as a priority in the 2015 Circular Economy Action Plan, to help European businesses and consumers to use resources more sustainably. The first-ever European Strategy for Plastics in a Circular Economy was adopted on 16 January 2018. Better design of plastic products, higher plastic waste recycling rates, more and better quality of recycle will help boost the market for recycled plastics. This strategy is part of Europe’s transition towards a circular economy and will also contribute to reaching the Sustainable Development Goals, the global climate commitments and the EU’s industrial policy objectives [1].

In light of this general problem, bioplastics—polymeric materials derived from renewable sources—now have their chance. They show the advantage of reduced dependence on fossil-based sources, and in most cases, they show complete biodegradability. Different types of bioplastics are known, mostly based on the general families of carbohydrates and proteins. These materials still show several technological limitations that hinder more widespread use. They are difficult to process, brittle, too sensitive to water and poorly resistant to high temperatures. Biodegradable polyesters such as poly-lactic acid (PLA) show better performances, but they are only hemi-synthetic. Finally, bacterial polyesters such as polyhydroxyalkanoates (PHAs) are an interesting class of bioplastics naturally

produced by a variety of microorganisms [2,3]. PHAs are linear biodegradable polyesters that can be produced by different types of bacteria as energy and carbon storage materials. PHAs are good candidates for the substitution of conventional oil-based technical plastics. Compared to conventional synthetic polymers, PHAs show obvious ecological advantages since they are completely biodegradable and nontoxic [4,5] and can be produced from renewable sources, such as glucose or sugar beet bagasse.

PHAs are composed of hydroxyalkanoic acid monomers with a straight or branched chain containing aliphatic or aromatic side groups [3]. Several metabolic pathways are described for the production of PHAs in bacteria; these processes usually involve acetyl-CoA or acyl-CoA as intermediate steps [6]. PHAs' biodegradation is performed by a microorganism that produces PHA depolymerase, an enzyme that allows the conversion of PHAs to water and carbon dioxide or methane [7].

Different types of PHAs have been bio-produced and many others are currently under investigation. Among them, polyhydroxybutyrate (PHB) and poly(3-hydroxybutyrate-co-3-hydroxyvalerate) P(HB/HV) copolymers are the most widely known. PHB is highly crystalline, stiff and brittle, with a melting temperature of 175 °C; P(HB/HV), instead, is more flexible and impact resistant according to the content of hydroxyvalerate (HV) units.

In PHAs mixed microbial cultures (MMC) process, polymer production and composition strongly depend on the operating parameters, mainly on the composition of the feeding solution and pH [8]. Few studies [9,10] have described the effect of pH on the rate and yield of polymer accumulation, typically indicating a higher production when the pH is controlled between 8 and 9. Along this line, it was found [11] that pH also plays a pivotal role on the regulation of the ratio between HB and HV monomers. This finding is particularly relevant since the pH can be used as a tool to regulate the HV content in the P(HB/HV) copolymer, regardless of the composition of the feeding. Moreover, to optimize the control of polymer composition, an innovative strategy could be to simultaneously regulate the pH as well as the rate of addition of the feeding solution in the PHAs accumulation stage. Indeed, when precursors of HV formation (i.e., propionic and valeric acid) [12] are depleted in the medium, only the HB monomer can be produced.

Data regarding PHA producing bacteria and assays for their identification were described in depth in Frison et al., 2021. The variation of the microbial community and identification of specific strains involved in the PHA production process were investigated through polymerase chain reaction denaturing gradient gel electrophoresis (PCR-DGGE) and fluorescence in situ hybridization (FISH) analyses. The results confirmed a relative abundance of the genera *Thauera* (58.2 ± 11.1%), *Paracoccus* (19.1 ± 5.2%) and *Azoarcus* (17.4 ± 4.9%) [13].

Activated sludge from wastewater treatment plants (WWTPs) is a known source of PHAs-storing organisms [14]. PHAs production from mixed cultures is accomplished by a sequence of operations: (i) acidogenic fermentation to produce volatile fatty acids (VFAs) from biodegradable organics; (ii) selection of PHAs storing biomass in a sequencing batch reactor (SBR); (iii) batch step to maximize PHAs accumulation in the bacteria cells. The carbon limitation strategy under feast and famine conditions has been found to be favorable for the enrichment and long-term cultivation of PHA-producing bacterial communities, while nitrogen limitation is a successful strategy that can be employed to accomplish high PHAs contents during the PHAs production step [15]. However, these processes are completely aerobic and energy-intensive; it is estimated that approximately 39 MJ are needed to produce 1 kg of PHAs when aerobic accumulation is employed [16,17].

Therefore, it would be desirable to develop more economic ways for PHAs production and new business models for their deployment. One strategy could be the integration of PHAs production within existing waste-treatment processes, i.e., by eliminating the cost of the carbon source while synergistically enhancing the efficiency of the waste-treatment process itself.

An attractive way would be to integrate microalgal culturing into the wastewater treatment process [18]. However, this strategy will require a redesign and upgrading of the

current treatment plants by substituting the current biological unit with a microalgae-based one, which also requires adequate climatic conditions (see for instance the demonstrative installation of the ALL GAS project located in Chiclana in the South of Spain [19]). In contrast, solutions that integrate microalgae as a side stream process (i.e., in the so-called sludge line) have been proposed. Microalgae are grown by profiting of nutrient-rich side-stream (the liquid fraction of digestate) and CO<sub>2</sub> rich-streams coming from anaerobic digestion, either as off-gasses from biogas combustion or as CO<sub>2</sub> from biogas upgrading [20,21]. In this scenario, the microalgae-based nitrogen conversion would reduce the N load to be dealt with by the main activated sludge treatment, thus reducing the associated energy cost. At the same time, microalgal biomass could be sent to the local anaerobic digester to be converted into biogas thus improving the energy balance of the plant or could enter additional process units to be converted into more valuable products such as biofillers [22] or biofertilizers [23]. Moreover, microalgal biomass is a potentially exploitable source for the production of VFA-rich streams via acidogenic fermentation. An interesting aspect is the production of propionic and butyric acid that is expected from the fermentation of protein-rich substrates such as microalgae [24], which could obtain a wide range of PHA copolymers. However, the production of VFA through fermentation of microalgal biomass and the consequent conversion to PHAs has received little attention and needs further study [25–27].

In this paper, a process chain (Figure 1) is considered for its potential to improve the recovery of materials from WWTP in an energy-effective way, including:

- microalgal culturing on the liquid phase of digestate, which is rich in nitrogen and phosphorus and on CO<sub>2</sub> from biogas upgrading, thus converting solar energy and inorganic nutrients into microalgae biomass via photosynthesis;
- acidogenic co-fermentation of waste activated sludge and microalgae to produce a fermented liquor rich in volatile fatty acids (VFA);
- separation of the nutrients (N and P) released during the fermentation process to produce struvite, a slow-release fertilizer;
- biological conversion of the VFA mixture into bioplastics (PHAs) by using selected PHAs storing biomass through feast/famine strategy and recovery from PHAs from the bacterial biomass.

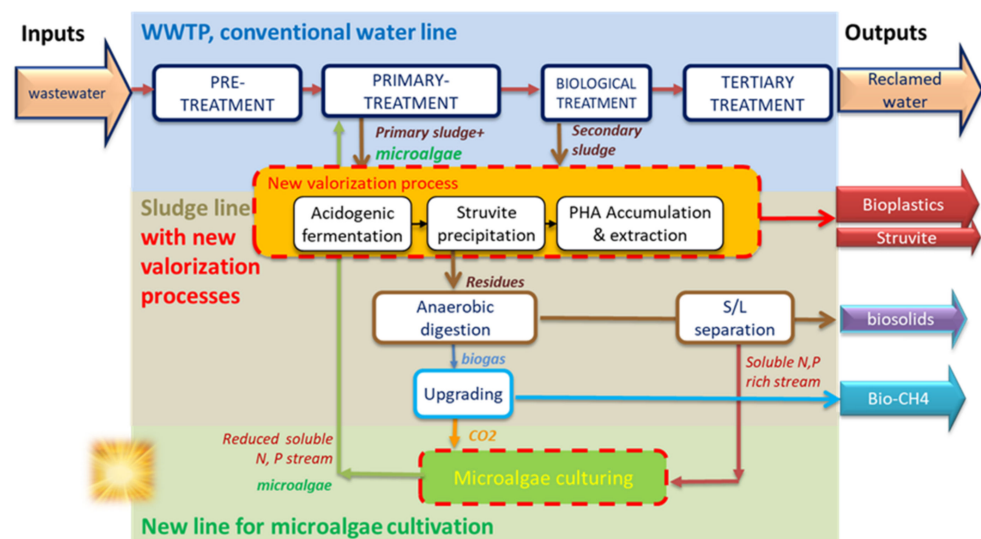


**Figure 1.** Typical WWTP scheme and additional treatments for resource recovery from wastewater as red dashed items: (i) Microalgae culturing on the liquid fraction of digestate and CO<sub>2</sub> from biogas upgrading; (ii) waste sludge and microalgae valorization to bioplastics and struvite.

The main advantages of this process chain include: (i) the amount of biomass that can be fermented to VFA for struvite and bioplastics production is increased, compared

to the fermentation of the sole waste sludge; (ii) the nutrient loads that are returned to the waterline are reduced, thus limiting the energy/chemical demand; (iii) the proposed technology is suitable for being integrated into existing or new WWTPs, even under sub-optimal climatic conditions for microalgae culturing. Indeed, the microalgae treatment is not responsible for meeting the final effluent quality, relieving the consequences of the seasonality and climatic dependence, which is one of the main constraints in microalgae-based treatment. The above-described treatment chain was tested at the laboratory- and pilot-scale up to the biopolymers and biocompounds characterization (composition and structural features) with a view to their potential marketability. The scheme of this process is shown in Figure 1.

## 2. Materials and Methods

### 2.1. Co-Fermentation Tests of Waste Sludge and Microalgal Biomass

The sludge and the inoculum used for batch tests were sampled from the WWTP of Sesto San Giovanni (Milano, Italy); their main chemical characteristics are listed in Table 1. The waste sludge is a mixture of primary (above 80% on mass basis) and secondary sludge, while the inoculum was taken at the outlet of the anaerobic digester and pre-treated at a temperature of 90 °C for 1 h to inactivate methanogens and thus reduce the conversion of VFAs into methane. The microalgal biomass was collected from a pilot-scale raceway pond installed outdoor at the WWTP of Bresso-Niguarda (Milano, Italy). The pilot-scale raceway had a surface area of 6 m<sup>2</sup> with a water depth of 0.2 m, and it was continuously fed with the liquid fraction from centrifugation of digestate (centrate). The algal biomass was mainly composed of green algae (*Chlorella* spp. and *Scenedesmus* spp.). Table 1 shows the main characteristics of the algal biomass after harvesting by centrifugation. A comprehensive description of the centrate and of the pilot plant characteristics and performances is beyond the scope of this study, but a detailed discussion has been previously published [28,29].

**Table 1.** Main characteristics of substrates used in co-fermentation tests.

		Sludge		Microalgae
		Waste Sludge	Inoculum	Mixed Community
pH	-	5.59 ± 0.11	7.3 ± 0.1	6.93
Total Alkalinity (TA)	mgCaCO <sub>3</sub> /L	1224 ± 81	3930 ± 1160	n.a.
Total Volatile Fatty Acids (TVFAs)	gCOD/L	1.70 ± 0.45	159 ± 39	n.a.
Total Solids (TS)	g/kg	38 ± 2.94	23.7 ± 6.4	50
Volatile Solids (VS)	g/kg	29.3 ± 0.94	15.7 ± 4.5	40
Total Suspended Solids (TSS)	g/kg	n.a.	16.3 ± 5.7	n.a.
Volatile Suspended Solids (VSS)	g/kg	n.a.	11.4 ± 4.1	n.a.
Soluble COD (SCOD)	g/kg	3 ± 0.78	2 ± 1.4	980
Total COD (TCOD)	g/kg	40 ± 2.4	n.a.	n.a.
Ammonium (NH <sub>4</sub> -N)	mgN/L	117 ± 6	681 ± 195	25
Nitrite (NO <sub>2</sub> -N)	mgN/L	n.a.	n.a.	n.a.
Nitrate (NO <sub>3</sub> -N)	mgN/L	n.a.	0.59	n.a.
Phosphate (PO <sub>4</sub> -P)	mgP/L	16 ± 5.2	n.a.	6

Mesophilic (37 °C) co-fermentation batch tests were performed in glass bottles (330 mL) closed with rubber septa with a working volume in the range of 200–250 mL. To ensure anaerobic conditions, the headspace of each bottle was flushed with N<sub>2</sub>. Table 2 summarizes the initial conditions for all the batch tests. Only test B1 was performed without inoculum. All substrate mixtures had a total initial VS concentration of 30 g/L and different

proportions of algae and waste sludge, while the inoculum had a total initial VS concentration of 10 g/L. The volume of biogas produced in a certain interval of time was indirectly quantified by measuring the pressure in the headspace of the bottle through a digital manometer (Keller LEO 2). pH, VFAs concentration and composition were measured at the beginning of the experiment (0) and after 3, 7 or 8, 10 or 11 days. Concerning test B1, the same parameters were also measured after 18 and 22 days. The biogas composition of each bottle was also detected on day 22 for B1 tests and days 7 and 10 for B2 tests.

**Table 2.** Initial conditions of batch co-fermentation tests.

		B1	B2.1	B2.2	B2.3	B2.4	B2.5
pH	-	5.5	6.5	6.9	6.5	6.7	7
Waste sludge	% *	100	100	90	75	50	0
Algae	% *	0	0	10	25	50	100

\* Percentage referred to the total volume of the sludge and algae mixture.

The degree of acidification (Da) was evaluated as the ratio between the fermentation products and the VS of the initial substrate. Fermentation products include VFA and methane, quantified as COD.

## 2.2. Production and Characterization of PHAs

The PHAs were produced from a mixed microbial culture selected under feast and famine conditions in a sequencing batch reactor (S-SBR) with a total volume of 30 L. During the experiment, the feast/famine ratio was maintained lower than 0.2 min/min, since this had been reported as a limit value to sustain a microbial consortium that will accomplish excess PHAs storage overgrowth [12]. The selection SBR (S-SBR) was not inoculated with a specific strain as the inoculum was conventional activated sludge from a municipal WWTP. The selective pressure of the operating conditions applied in the S-SBR led to the relative abundance of three main genera of PHA-producing bacteria, as reported in a previously published study [13].

Oxygen was provided by a blower (Scubla, Italy) and ultrafine bubble diffusers placed in the bottom of the tank. The blower was controlled to maintain a DO concentration of  $2 \pm 0.2$  mgO<sub>2</sub>/L. At the beginning of the cycle (feast phase), the carbon source was fed with a peristaltic pump according to an organic loading rate of 1.58 gCOD/m<sup>3</sup> day [30]. The excess sludge produced in the S-SBR was used as inoculum to produce PHAs according to a multiple pulse feeding strategy [31]. The accumulation reactor (A-SBR) consisted of a stainless-steel tank, with a volume of 30 L, which operated as a fed-batch reactor. The reactor was equipped with a DO probe (Hach-Lange, Germany) and ultra-fine bubble diffusers (Scubla, Italy) placed at the bottom of the tank, which provided oxygen through a centrifuge blower (Scubla, Italy) at a flow rate of 200 l/min. The excess sludge from the S-SBR was transferred to the A-SBR at the end of the cycle. The accumulation trials lasted between 6 and 7 h and the carbon source was added based on feed-on-demand strategy using DO as a control parameter [32], according to an initial COD concentration of around 0.7–1.2 g COD<sub>VFA</sub>/L to prevent any substrate inhibition as reported by Valentino et al. [31]. The PHA-rich biomass was obtained with VFAs as substrate with different ratios of acetic acid (HAc) to propionic acid (HPr). In particular, the following ratios HAc:HPr were studied: 60:40, 50:50, 30:70, 0:100.

PHAs were recovered by extraction with a VELP® Scientifica SER 148 solvent extractor: 2g of biomass were put in a cellulose thimble (Whatman 603, 33 × 100 × 1.5mm) and, for each, 60 mL of chloroform (Sigma-Aldrich) were used. The operating conditions of the extractor were: 90 min of immersion, 120 min of washing and 5 min of recovery.

Figure 2 shows the scheme of the process here described.

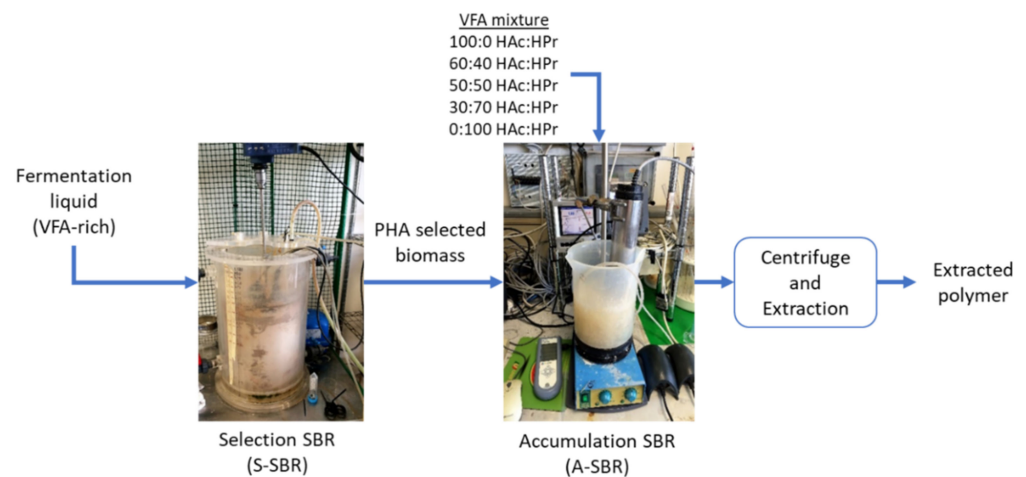


**Figure 2.** Scheme of the apparatus for the production of PHAs.

Figure 2 shows a scheme that includes the selection of PHA storing bacteria, the accumulation, centrifugation and extraction of the polymer.

### 2.2.1. Nuclear Magnetic Resonance (NMR)

The composition and microstructure of the extracted and fractionated PHAs were determined using  $^{13}\text{C}$ -NMR and  $^1\text{H}$ -NMR spectroscopy. Spectra were recorded in deuteriochloroform ( $\text{CDCl}_3$ ) ( $10\text{ mg mL}^{-1}$  for  $^1\text{H}$ -NMR and  $30\text{ mg mL}^{-1}$  for  $^{13}\text{C}$ -NMR) at  $25\text{ }^\circ\text{C}$  on a Bruker SampleXpress spectrometer. Relative peak intensities for this purpose were analyzed using the peak fitting program MNova. Peak shifts were referenced to  $\text{CDCl}_3$  peak at  $7.26\text{ ppm}$  ( $^1\text{H}$ -NMR) and  $77\text{ ppm}$  ( $^{13}\text{C}$ -NMR). From  $^{13}\text{C}$ -NMR analysis, the chemical compositional distribution of PHAs was determined. Diad sequence analysis was used to assess the extent of deviation of the PHBV copolymer composition from the statistically random Bernoullian compositional distribution by evaluating the parameter  $D$ , defined by Kamiya et al. [33].  $D$  is given by:

$$D = (F_{\text{BB}} \cdot F_{\text{VV}}) / (F_{\text{BV}} \cdot F_{\text{VB}}), \quad (1)$$

where  $F_{\text{BB}}$ ,  $F_{\text{VV}}$ ,  $F_{\text{BV}}$  and  $F_{\text{VB}}$  are the molar fractions of the  $\text{HB}^*\text{HB}$ ,  $\text{HV}^*\text{HV}$ ,  $\text{HB}^*\text{HV}$  and  $\text{HV}^*\text{HB}$  diad sequences, respectively. In brief, for a statistically random copolymer  $D$  is equal to 1; for a block copolymer or a mixture of copolymers  $D$  is greater than 1, and for an alternating copolymer  $D$  is less 1.

### 2.2.2. Gel Permeation Chromatography (GPC)

Molecular weight measurements on extracted and fractionated PHA samples were performed using a Waters 510 Gel Permeation Chromatography (GPC) apparatus working in tetrahydrofuran (THF) at  $40\text{ }^\circ\text{C}$ , equipped with a set of Ultrastaygel<sup>®</sup> columns and a Waters 410 differential refractometer as detector. The calibration was performed with monodisperse fractions of PS.

### 2.2.3. Dilute Solution Viscometry

Dilute solution viscometry was carried out for one extracted PHA batch, insoluble in THF for GPC analysis. The sample was dissolved in  $\text{CHCl}_3$  and the efflux time of the solution from a capillary in calibrated glass was measured at  $30\text{ }^\circ\text{C}$ . The intrinsic viscosity was computed with a double extrapolation at zero concentration of two semi-empirical equations (Huggins and Kraemer equations). Then, the Mark-Houwink empirical equation was exploited to obtain the viscosity average molecular weight ( $M_{\eta}$ ) assumed to be equal to the weight average molecular weight  $M_w$  as a first approximation. The empirical constants of PHB in  $\text{CHCl}_3$  at  $30\text{ }^\circ\text{C}$  were used, with  $K = 0.0118\text{ mL/g}$  and  $\alpha = 0.78$  [34].

### 2.2.4. Differential Scanning Calorimetry (DSC)

Thermal properties analysis was carried out using DSC for extracted and fractionated PHAs. All runs were performed on 5–10 mg samples in a nitrogen atmosphere. The data obtained were used to calculate the glass transition temperature ( $T_g$ ), crystallization temperature ( $T_c$ ), cold crystallization temperature ( $T_{cc}$ ), melting point ( $T_m$ ) and fusion enthalpies ( $\Delta H_m$ ).

The DSC thermal history consisted of: (i) a first heating run from 25 °C to 200 °C (20 °C min<sup>-1</sup>); (ii) a cooling step from 200 °C to 170 °C at 20 °C min<sup>-1</sup>, from 170 °C to 0 °C at 10 °C min<sup>-1</sup> to stimulate the polymer crystallization, from 0 °C to -50 °C at 20 °C min<sup>-1</sup>; and (iii) a second heating run from -50 °C to 200 °C (20 °C min<sup>-1</sup>).

### 2.2.5. Solvent/Non-Solvent Fractionation

One batch among the extracted PHAs was compositionally fractionated with a CHCl<sub>3</sub>/n-hexane mixed solvent at ambient temperature. A mass of 2.0 g of sample was dissolved in 200 mL CDCl<sub>3</sub>, and 1 mL aliquots of n-hexane were progressively added with gentle agitation. At the first sign of cloudiness, the mixture was allowed to stand for 24 h and the precipitate was obtained by centrifugation at 4000 rpm for 10 min. This procedure was repeated until the further addition of n-hexane was unable to produce any more precipitate. The obtained fractions were dried in a vacuum oven at 50 °C for at least 24 h.

### 2.2.6. PHA from a Mixed Sludge/Microalgae Feedstock

To properly understand the chemical and physical nature of a PHA produced in a real-case scenario, the MMCs were fed with a mixture of pure VFA mimicking the composition of what could be obtained by the co-fermentation of waste sludge and microalgal biomass. The single VFA were mixed with the following ratio: 37% of acetic acid (Hac), 30% of propionic acid (HPr), 16% of butyric acid (HBu) and 17% valeric acid (HVa).

## 3. Results

### 3.1. Batch Co-Fermentation Tests

Batch tests revealed the potential VFA production from the tested substrates. Results are summarized in Table 3 and Figure 3, where pH at the beginning/end of the experiment, the  $D_a$  value (in gCOD/gVS) and the VFA speciation are reported. A first comparison can be made between tests performed with (B2.1) and without (B1) inoculum. The degree of acidification in B2.1 was much lower than that in B1 likely because of the higher operational pH. The  $D_a$  of B1 was 0.3 on day 10, and even higher (0.47) on day 22 when a higher pH of 6.1 was observed, suggesting that methanogenesis took place in the last week of this batch tests. In the B2 set, the inoculum was used to accelerate the fermentation process and shorten the test duration. In this set, low but measurable methane production was observed. A methane percentage in the biogas between 30 and 40% was measured in all bottles on the day of maximum VFAs production. However, the final methane yield remained below 5(%) as COD, suggesting that the inoculum pretreatment slowed down the methanogenic activity but did not fully prevent it.

**Table 3.** Main results of batch co-fermentation tests.

	Day 0		Day 3		Days 7/8		Days 10/11	
	pH	$D_a$	pH	$D_a$	pH	$D_{a,B}$	pH	$D_a$
B1	5.50	0.080	5.60	0.200	5.55	0.230	5.40	0.300
B2.1	6.50	0.067	6.90	0.100	6.97	0.150	6.60	0.115
B2.2	6.90	0.033	6.70	0.100	6.92	0.180	6.70	0.170
B2.3	6.50	0.083	6.70	0.080	6.95	0.140	6.70	0.150
B2.4	6.70	0.080	6.70	0.076	6.98	0.120	6.70	0.140
B2.5	7.00	0.020	7.00	0.030	7.10	0.093	6.70	0.075

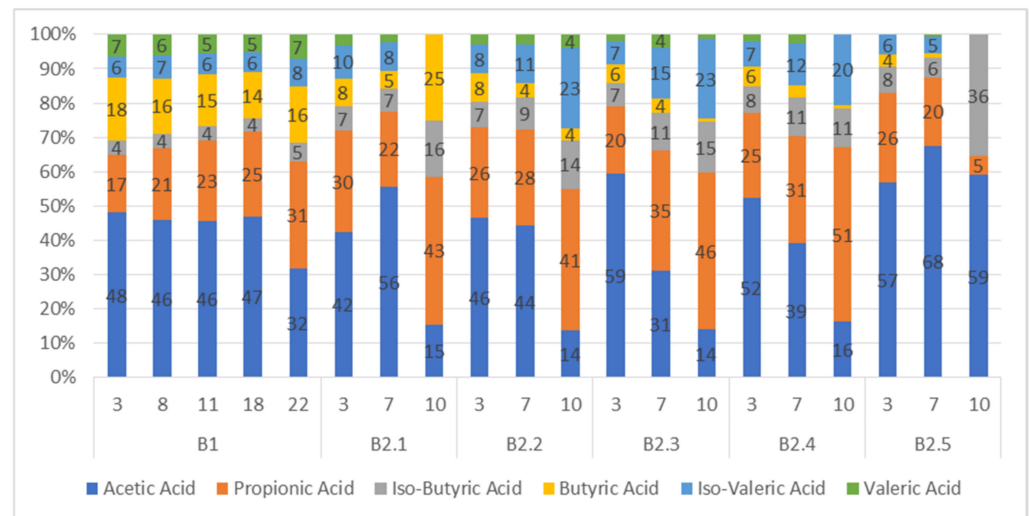


**Figure 3.** VFAs speciation of fermented liquid (as equivalent COD) at different sampling times.

In Figure 3, the VFA composition is reported. Acetic acid was always the main VFA component at the beginning of the test (day 3), while its percentage was generally lower at the end of the acidification tests as a consequence of the onset of methane production. Acetic acid conversion to methane was slower in test B1, where no anaerobic inoculum was used, and in B2.5, where algae were the sole substrate and the overall acidification process was slightly less efficient, as suggested by the lower degree of acidification, thus resulting in delayed methane production.

Co-fermentation tests were performed to identify possible synergistic or competitive effects between the two substrates, namely waste sludge and microalgae. Starting from the VFAs concentration obtained in bottles with only waste sludge and microalgae (B2.1 and B2.5), the expected total VFAs' concentrations in the other bottles were computed, assuming an additive contribution of the co-fermented substrates. These expected values were then compared to those obtained experimentally in the co-fermentation bottles for the day of maximum VFA accumulation. Note that in this evaluation the amount of biogas produced was accounted for as extra acetic acid. Results showed that, though concentrations of VFAs higher than the theoretical ones were detected for two of the three mixtures (by 22% and 12% for the mixtures B2.2 and B2.3, respectively), the co-fermentation of these two substrates leads to very limited synergistic or competitive effects.

The effect of the composition of the VFA-rich liquor on the PHA production was then tested. Focusing on varying the proportion of the two main VFAs that were found in co-fermentation tests. For each substrate composition as HAc:HPr studied, except for 60:40 HAc:HPr, two batches of PHAs were produced at different times, approximately at a distance of two months from one another (named batch I and II).

After solvent extraction using chloroform, the extracted PHA masses were measured, and dry weights were calculated. The extraction process showed a maximum of 26 wt% for the first batch of PHA produced using 50:50 HAc:HPr as a carbon source.

### 3.2. Compositional Analysis

Compositional analyses, carried out by  $^1\text{H-NMR}$ , highlighted that all the extracted PHA were PHBV copolymers, with a variable content of HV units. To highlight the qualitative trend, the results are reported in Figure 4.

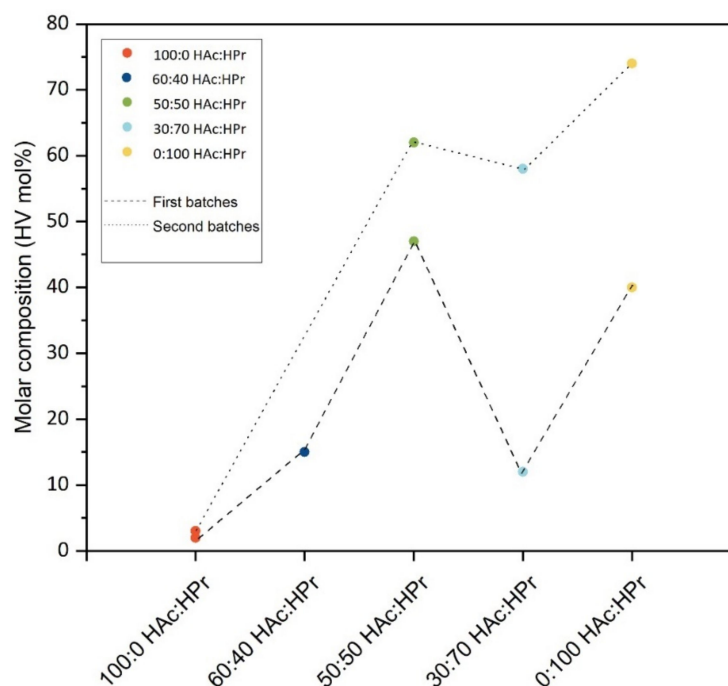


**Figure 4.** Molar composition (HV%) of extracted PHAs versus substrate composition (HAc:HPr) evaluated by  $^1\text{H-NMR}$ .

Using HAc only as a substrate, the PHAs obtained are copolymers, with a minimal amount of HV, equal to 2 mol% and 3 mol%. By increasing the HPr relative content over the HAc, the HV units tend to generally grow as reported by both the dashed (first batches) and dotted (second batches) lines and reach a maximum value of 66 mol% when only HPr was chosen.

However, this trend has some exceptions: firstly, it is evident that the molar content of HV units decreased using a substrate 30:70 HAc:HPr with respect to the 50:50 ratio, for both batches; secondly, the use of the same HAc:HPr ratio in the two batches produced copolymers that had a highly different content of HV units.

The exception found that using as a substrate 30:70 HAc:HPr could be related to the poor acclimation of the PHA storing biomass to uptake propionic acid faster than acetic acid. Indeed, this composition of VFA differed significantly from the fermentation liquid (VFA-rich) used during the selection of PHA storing bacteria, which was characterized by a higher HAc:HPr ratio.

The comonomer sequence distribution in the copolymeric chains was evaluated by  $^{13}\text{C-NMR}$ . For the samples rich in HB units (97 mol% and 98 mol%), obtained by a substrate of 100:0 HAc:HPr, a quantitative evaluation of the relative intensities was not possible.

### 3.3. Molecular Weight Measurement

An accurate determination of the true molecular weight requires a dilute solution viscometry measurement. However, the Mark-Houwink parameters have only been reported for the PHB homopolymer. Therefore, in this study, molecular weight measurements of extracted PHAs were conducted by dilute solution viscometry only for PHA produced with 100:0 HAc:HPr. In fact, due to its limited HV unit content (2 mol%), it was possible to estimate the molecular weight with an acceptable error, using the Mark-Houwink parameter for the homopolymer. For all the other PHAs, being copolymers at high content of HV units, GPC was used, with the advantage of having more complete information.

For the first batch of PHA produced with 100:0 HAc:HPr, the computed viscosity average molecular weight,  $M_{\eta}$ , that corresponds to the weight average molecular weight  $M_w$  in first approximation, is  $M_{\eta} \approx M_w = 7.47 \cdot 10^5$  Da. Such high  $M_w$  was expected: it is

known that the molecular weight of PHAs synthesized by biological means is much higher than that achieved chemically [35].

GPC analyses were performed on all the other batches of PHAs. The results are reported in Table 4 in terms of weight average molecular weight  $M_w$ , number average molecular weight  $M_n$  and polydispersity index PDI. By averaging the values for all the GPC measurements, it is obtained:

$$M_w = (2.45 \pm 0.51) \cdot 10^5 \text{ Da}$$

$$M_n = (1.50 \pm 0.52) \cdot 10^5 \text{ Da}$$

$$PDI = 1.75 \pm 0.52$$

**Table 4.** Extracted polymer normalized by the dry weight of the biomass, molar composition evaluated by  $^1\text{H-NMR}$ , parameter D evaluated by  $^{13}\text{C-NMR}$ , weight average molecular weight  $M_w$ , number average molecular weight  $M_n$  and polydispersity index PDI evaluated by GPC or dilute solution viscometry (\*) of the extracted PHAs labeled by HAc:HPr ratio and batch.

HAc:HPr—Batch Label	Extracted Polymer	Molar Composition	D	Mw	PDI
[g-COD/L:g-COD/L]	[wt%]	[HV mol%]		[10 <sup>5</sup> Da]	
100:0-I	15% ± 1%	2%	-	7.47 *	-
100:0-II	16% ± 1%	3%	-	-	-
60:40-I	8% ± 2%	15%	25.3	1.90	1.53
50:50-I	26% ± 2%	47%	35.2	2.45	1.33
50:50-II	16% ± 3%	62%	2.7	3.05	1.45
30:70-I	1% ± 0%	12%	13.2	1.95	2.78
30:70-II	15% ± 2%	58%	24.0	3.06	1.53
0:100-I	3% ± 1%	40%	46.0	2.18	1.66
0:100-II	10% ± 2%	74%	10.1	2.56	1.94

### 3.4. Thermal Analysis

DSC was carried out on PHAs samples to investigate their thermal behavior.

In Figure 5, the response to the heating scans is reported for the first batches of each ratio (HAc:HPr) of the tested carbon source. Scans are stacked in order of increasing HV content materials, going from the top (lowest content of HV) to the bottom (highest content of HV). The acquired data for all the extracted PHAs are summarized in Table 5, reporting the melting peaks with the associated enthalpy of fusion. It should be noted that the first heating scan was used for the determination of  $T_m$  since in the second heating scan the lower melting components were no longer evident due to insufficient time for crystallization.

Focusing on the thermogram obtained from the first heating scan (Figure 5a) on the as-produced PHAs, the complexity in the thermal response of the materials, which appear to be semi-crystalline, is evident. In particular, PHAs with a low content of HV show a single melting peak at a temperature above 160 °C; by increasing the HV unit content, other melting peaks were evidenced. During the second heating scan, instead, independently of the copolymer composition, all samples showed a single melting point at the same temperature interval, corresponding to the highest melting peak of the first heating scan. The lower melting components were no longer able to crystallize due to insufficient time, implying slow crystallization kinetics associated with those domains.

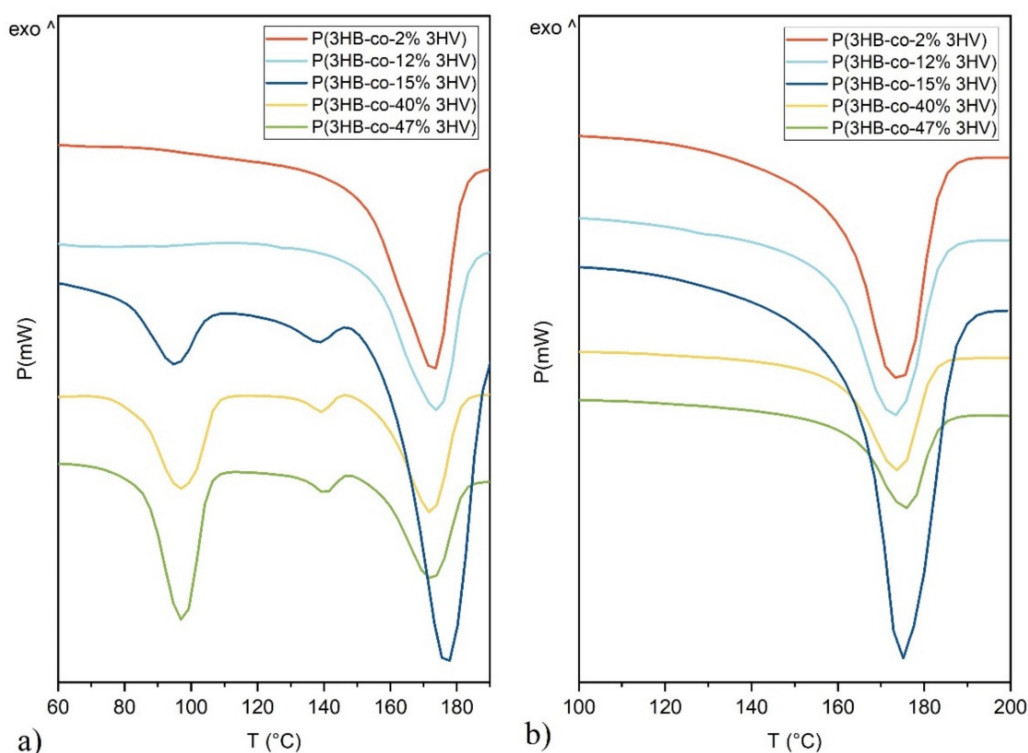


**Figure 5.** Thermograms acquired by DSC scan for PHAs of the first batches: Left (a): first heating scan; right (b): second heating scan. Exo ^ indicates the direction of exothermic flow.

**Table 5.** Results of thermal analyses by DSC for extracted PHAs. The melting temperatures  $T_m$ , distinguished for  $T < 160$  °C and  $T > 160$  °C with the associated fusion enthalpies  $\Delta H_m$ , and the crystallinity degree  $\chi$  are obtained from the first heating scan; the crystallization temperature  $T_c$  and its crystallization enthalpies  $\Delta H_c$  refer to the cooling scan; glass transition temperatures  $T_g$  and cold crystallization temperature  $T_{cc}$  with its enthalpy  $\Delta H_{cc}$  were defined by the second heating scan.

HAc:HPr	HV	$T_m < 160$ °C	$\Delta H_m < 160$ °C	$T_m > 160$ °C	$\Delta H_m > 160$ °C	$\Delta H_m$ Total	$T_c$	$\chi$	$\Delta H_c$	$T_g$	$T_{cc}$	$\Delta H_{cc}$
[g-COD/L]	[mol%]	[°C]	[J/g]	[°C]	[J/g]	[J/g]	[°C]		[J/g]	[°C]	[°C]	[J/g]
100:0-I	2%	-	-	173	70	70	107	48%	66	9	-	-
100:0-II	3%	-	-	178	79	79	95	54%	63	8	-	-
30:70-I	12%	-	-	174	56	56	78	38%	40	-11/9	-	-
60:40-I	15%	95/138	11/2	177	68	64	94	55%	51	-12/9	-	-
0:100-I	40%	97/132	34/3	172	42	76	76	55%	25	-12/8	-	-
50:50-I	47%	98/140	44/1	175	31	75	88	55%	19	-10/8	-	-
30:70-II	58%	101/138	37/4	168	27	64	-	47%	-	-11/6	76	23
50:50-II	62%	97	45	164	1	46	-	35%	-	-6	-	-
0:100-II	74%	105	72	173	5	77	-	58%	-	-10	-	-

Figure 6 shows the melting temperatures and the corresponding enthalpy of the samples.

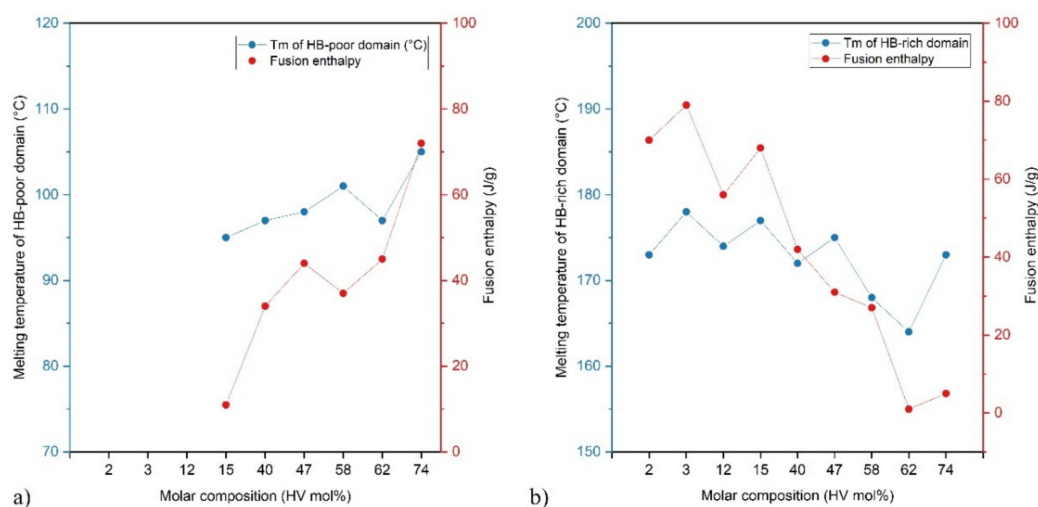


**Figure 6.** Melting temperature and fusion enthalpy trend versus the HV content in PHAs: Left (a): low-melting temperature fraction; right (b): high-melting temperature fraction.

In Figure 6, the trend in terms of  $T_m$  and the associated fusion enthalpy is shown for the two consistently evident phases. In fact, because of the clear distinction between the high- and low-melting peak regions observed, they have been considered as independent domains, with the enthalpies being separately determined.

The degree of crystallinity  $\chi$  was evaluated. One of the standard methods for determining  $\chi$  of semi-crystalline copolymers is by comparing the area of the melting peak ( $\Delta H_m$ ) with the melting enthalpy of a 100% crystalline material ( $\Delta H_m^\circ$ ):

$$\chi = \frac{\Delta H_m}{\Delta H_m^\circ}, \quad (2)$$

For PHBV, the value of  $\Delta H_m^\circ$  for the wide spectrum of composition observed in this work is not available in the literature. However, an estimate of the heat of fusion of an infinite crystal of PHB and PHV is reported to be 146 J/g ( $\Delta H_{m, PHB}^\circ$ ) and 131 J/g ( $\Delta H_{m, PHV}^\circ$ ), respectively [36].

These two values have been used to obtain a rough estimation of  $\chi$ . In particular, by considering the two well-defined melting peaks at  $T < 160^\circ\text{C}$  and  $T > 160^\circ\text{C}$ , the fusion enthalpy of the HB-poor domain ( $T < 160^\circ\text{C}$ ) was normalized to  $\Delta H_{m, PHV}^\circ$ , while the fusion enthalpy of the HB-rich domain ( $T > 160^\circ\text{C}$ ) was normalized to  $\Delta H_{m, PHB}^\circ$ . This calculation assumes, as a first approximation, that the limited amount of HB units in the HB-poor domain and the limited amount of HV units in the HB-rich domain would not excessively modify the values of  $\Delta H_{m, PHV}^\circ$  and  $\Delta H_{m, PHB}^\circ$ .

A specific trend is not observed: the crystallinity seems to be independent of the HV unit content.

### 3.5. Solvent/Non-Solvent Fractionation

To further validate the result that extracted PHAs in this study are mixtures of random copolymers or block copolymers, and specifically analyze the properties of the different phases, a solvent/non-solvent fractionation was carried out. This process was performed on a single batch, which showed high parameter D and two well-defined melting peaks in DSC analyses. In particular, P(3HB-co-58% 3HV), produced by a substrate of 30:70 HAc:HPi (second batch), was selected. The solvent/non-solvent fractionation resulted in the separation of four fractions, which were analyzed in terms of  $^1\text{H-NMR}$ ,  $^{13}\text{C-NMR}$ , GPC and DSC. The four fractions obtained are labeled with a number from 1 to 4, moving from the firstly precipitated fraction to the last one. The results are summarized in Table 6.

**Table 6.** Mass fraction, molar composition (HV%), melting temperatures  $T_m$  and fusion enthalpies  $\Delta H_m$  of the fractions obtained by solvent/non-solvent fractionation of P(3HB-co-58% 3HV).

Fraction	Mass Fraction	HV Molar Composition	D	Mw	Mn	PDI	Tm	$\Delta H_m$
	[wt%]	[HV mol%]		[ $10^5$ Da]	[ $10^5$ Da]		[ $^{\circ}$ C]	[J/g]
1	11%	-	-	-	-	-	172	59
2	29%	11%	18.8	3.13	2.57	1.22	150/169	65
3	6%	35%	9.6	2.83	2.21	1.28	101/115/142/170	70
4	38%	88%	2.2	2.79	2.08	1.34	106	82

The PHA recovery resulted in 83 wt% of the polymer used in the procedure.

The precipitated fractions showed homogenous results in terms of molecular weights and PDI, coherent with the data reported in Table 4 for the extracted PHA used in the fractionation procedure. In particular, averaging the values among the fractions, the obtained results for the molecular weights and the polydispersity index are:

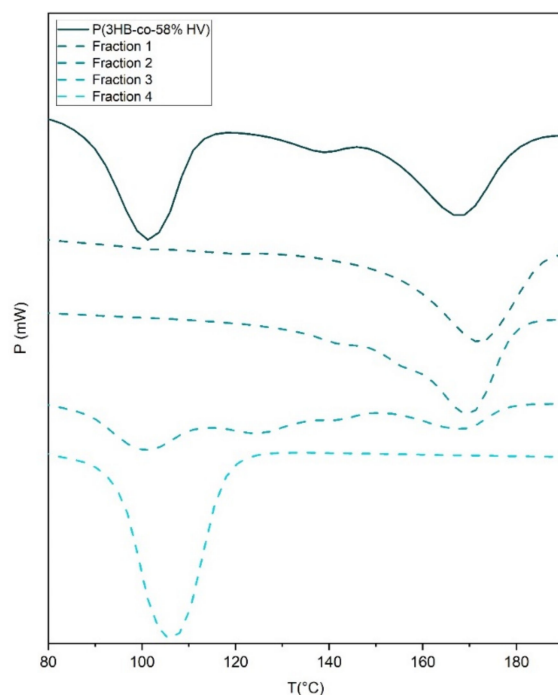
$$M_w = (2.92 \pm 0.19) \cdot 10^5 \text{ Da}$$

$$M_n = (2.29 \pm 0.25) \cdot 10^5 \text{ Da}$$

$$PDI = 1.28 \pm 0.06$$

It is to highlight that GPC requires the solubility of the polymer in THF, therefore the molecular weight measurement could not be carried out for fraction 1. On the contrary, the other fractions showed a better solubility, even though, for fraction 2 and fraction 3, the solution required filtration before being analyzed.

The first heating scan from the DSC analyses for the extracted PHA before being fractionated and the four fractions are reported in Figure 7.

**Figure 7.** Thermograms of the first heating scan acquired by DSC for the extracted PHA with a substrate 30:70 HAc:HPr (second batch) P(3HB-co-58% 3HV) before fractionation and for the four fractions obtained by solvent/non-solvent fractionation.

As expected, fraction 1, showed a high  $T_m$  (172 °C), which tends to confirm that it corresponds to pure PHB. Fraction 2, having 11 mol% HV, shows a shift at lower  $T_m$ : one peak is located at 169 °C with a shoulder, and another at 150 °C. Fraction 1 and partially fraction 2, together, constituted that part of the as-produced copolymer, which was named as HB-rich domain, had a  $T_m$  at 168 °C. Fraction 4, having 88 mol% of HV units, is the HB-poor domain, with a  $T_m$  of 106 °C, very close to the low melting peak of the as-produced copolymer, centered at 101 °C. An intermediate condition was found for fraction 3, showing a multi-melting peak ( $T_m$  at 101, 115, 142 and 170 °C) in the DSC thermogram. The presence of more than one peak suggests that this fraction itself was still constituted by different copolymers in terms of the HV:HB ratio. Indeed, the highest (170 °C) and the lowest (101 °C) peaks suggest that fraction 3 was partially constituted by those copolymers present in fractions 2 and 4, respectively. In addition, the peak at 142 °C could be attributed to the intermediate peak visible in the thermogram of P(3HB-co-58% 3HV) at 138 °C (referring to Figure 5). The peak at 115 °C, instead, was not visible in the thermogram in the material before being fractionated.

$^{13}\text{C}$ -NMR was carried out to define the sequence distribution diads and parameter  $D$  of the fractions obtained. As mentioned above, fraction 1 could not be analyzed due to the insolubility problem suggesting that it was constituted by HB units only (PHB), or with only trace amounts of HV. All the fractions showed  $D$  smaller than 24.0, which was the value obtained for the extracted PHA used in the fractionation procedure, but higher than 1.5, suggesting that they were still blends of copolymer or block copolymers. Fraction 2 and fraction 3 showed the highest values, 18.8 and 9.6, respectively. These values are coherent with the presence of more than one melting peak, as previously discussed (Table 5), and define the presence of blends of copolymers in these two fractions. Fraction 4, instead, showed a  $D$  of 2.2, which is smaller, coherently with the presence of a single melting temperature at 106 °C in the DSC analyses. However, since the value is larger than 1.5, it is possible to assume that fraction 4 is a block copolymer. The presence of blocks, in terms of long sequences of HV units in the polymeric chains, could justify the ability of these copolymers to crystallize. In fact, fraction 4 showed a large fusion enthalpy (82 J/g) associated with its melting peak, which suggests a high degree of crystallinity. As a rough approximation, assuming the melting enthalpy of a 100% crystalline of this material similar to that of PHV ( $\Delta H_{m, PHV}^\circ = 131 \text{ J/g}$ ) [37], the degree of crystallinity would correspond to 63%.

### 3.6. Characterization of a Reference PHA

The PHA obtained was characterized with the same methodologies of the previously described polymers. The composition analysis suggests a 41% molar concentration of HB and a 59% molar concentration of HV, with an alternate copolymer structure ( $D = 1.9$ ). GPC analysis provided the following parameter for the molecular weight:

$$\begin{aligned}M_w &= 2.75 \cdot 10^5 \text{ Da} \\M_n &= 2.04 \cdot 10^5 \text{ Da} \\PDI &= 1.34\end{aligned}$$

The thermal analysis showed two melting temperatures, one at 101 °C with an enthalpy of 52 J/g and one at 177 °C with a smaller enthalpy of 9 J/g. None of these peaks were able to crystallize and are not present in the second heating. The glass transition occurs at  $-7$  °C. The estimated degree of crystallinity is 46%. These results are not significantly different from those obtained with other PHAs, whose results are reported in Table 5. Therefore, it is possible to assume that the range of values obtained in the present study can be a useful basis to predict the possible outcomes of the final PHA.

## 4. Discussion

As for the co-fermentation of algal biomass with waste-sludge, results show that the composition of the other VFAs changed according to the nature of the substrate. Indeed,

the bottle fed on algae is the only one showing a relevant concentration of iso-butyric acid (up to 36%) while the percentages of propionic acid were negligible at day 10. On the contrary, waste sludge fermentation led to a relevant production of propionic acid. The co-digestion of algae and waste sludge led to the highest proportion of acetic and propionic acid (41–51%), indeed the highest percentage of propionic acid is being observed in B2.4, when similar amounts of algae and waste sludge were digested. Since pH was quite homogeneous in all B2 bottles, the observed differences in the VFAs speciation are to be attributed to the substrate nature. The composition of VFAs reflects the metabolic pathways of a specific carbon source. The microalgal biomass is typically rich in proteins (up to 52% on weight basis) and lipids (up to 23% on weight basis) [38,39]; this composition supports butyric and valeric acids production [40]. Carbohydrate-rich waste streams support acetic and propionic acid production [41]. It is also important to underline how operating conditions influence results: pH values slightly below neutral conditions (as in all these cases) promote acetic and propionic acids production [42]. As for VFA composition, at the end of all co-fermentation tests, the VFA mixture included all acids, with a more significant presence of valeric acids compared to the mono-fermentation trials. Results of these batch tests suggest that algal biomass and sludge can be effectively co-fermented with a final fermentation efficiency well in line with that computed from results from mono-fermentation tests; the final composition of the VFA mixture includes all acids with a prevalence of propionic and valeric acids.

As for PHA production by MMC, the PHA weight percentages obtained are not compatible with the recent results reported in the literature. In fact, PHA contents and production rates of MMC are reported to be comparable or superior to those of pure culture [43]. The reason for the low extraction PHA weight percentages can be related to the low a concentration in the initial biomass, due to the different mixture of VFAs used in the A-SBR compared with the S-SBR. The change in the type of carbon source could have negatively affected the uptake rate of the VFAs thus decreasing the final PHAs productivity.

Compositional analysis showed results in agreement with the literature [44–46], an increase in HV units in the copolymer has been observed by introducing HPr in the substrate. However, the first batches with 30:70 HAc:HPr and 0:100 HAc:HPr showed molar contents of HV of 12 mol% and 40 mol%, respectively, which are much lower if compared to the molar contents of the second ones, equal to 58 mol% and 74 mol%. Therefore, a certain variability in the batches produced in the same operational conditions has been observed. This fact, which is in line with some papers in the literature [36], is a well-known characteristic of biological syntheses, where many variables are involved in the process. In addition, it is relevant to highlight that PHAs were produced by a MMC whose precise composition can vary from one selection to another. Moreover, since a few months between the first and second batches had passed, variability in the bacteria population and the accumulation behavior was expected. Finally, it must be mentioned that the SBRs used for the accumulation procedure are located outdoors, and hence temperature variability can play an important role. As a result, variability in the produced PHAs is not a surprising fact. Obtaining PHAs had a very different composition, with HV units in the copolymer ranging from 2 mol% to 74 mol%; they had the positive effect of making the investigation of property variations for a large spectrum of the copolymer composition possible.

The microstructural analysis showed that, in all cases, the quantitative evaluation resulted in  $D$  much larger than 1.5, which is the value proposed by Kamiya et al. [33] above which the material is a mixture of random copolymers and/or “blocky” copolymer. However, it should be noticed that the entity of this phenomenon is variable:  $D$  ranges between 2.7 and 46.0. In particular, PHAs obtained by substrates 50:50 HAc:HPr (second batch), 0:100 HAc:HPr (second batch) and 30:70 HAc:HPr (first batch) have  $D$  equal to 2.7, 10.1 and 13.2, respectively. These are the lowest values obtained, smaller than all the others, which in some cases are higher than an order of magnitude.

These observations are consistent with other studies [33,36,46–48] dealing with microbial polyester produced by MMC. In particular, Albuquerque et al. [48] through in

situ analysis of substrate uptake capabilities using microautoradiography-fluorescent in situ hybridization, found that MMC enriched and fed on mixed feeds are composed of multiple populations specialized in the uptake of different substrates. Hence, the formation of polymer blends is not an unexpected outcome.

GPC analyses showed that the molecular weights, with  $M_w$  ranging from  $1.90 \cdot 10^5$  Da and  $3.06 \cdot 10^5$  Da are in line with the values in the literature [37,49]. The polydispersity indices show a medium-narrow size distribution, where all PDI are less than 2, with a single exception for the PHA of the second batch with the substrate 30:70 HAc:HPr having instead a value of 2.78. However, the exhibited variability is expected and found in many other studies [46,50]. In fact, in a bio-synthetic process of polymerization of an MMC, many variables are involved.  $M_w$ ,  $M_n$  and PDI did not show a specific trend according to the copolymer composition.

Thermal analysis presents a peculiar behavior that is justified by the presence of complex blends, of high- and low-melting copolymers fractions, as previously observed with  $^{13}\text{C}$ -NMR analyses, with micro- and/or macro-phase separation leading to domains of differing composition. The parameter D shows values (Table 4) that are coherent with the results of thermal analyses.

This complex result is not an isolated case: many as-produced microbial PHA polymers consist of blends of copolymers of different compositions and several studies exploring the effect of deliberate blending of different random copolymers of PHAs on polymer properties were carried out [37]. It is well-established that pure PHB and pure PHV are immiscible in the melt: blends of PHB and PHV contain phase-separated domains in the melt, which crystallize as PHB and PHV type spherulites, respectively [51]. As a result, the different domains formed melt phases at different temperatures, giving a multi-melting peak curve at the heating scan.

Melting temperatures are not affected by the average composition but the fusion enthalpies show a clear trend. In fact, as expected, by increasing the content of HV units, the enthalpy increases for peaks at a temperature below  $110\text{ }^\circ\text{C}$ , which were attributed to the HB-poor domain in the copolymer, hence, rich in HV units. The enthalpy gradually decreases for peaks at a temperature above  $160\text{ }^\circ\text{C}$ , which were attributed to the HB-rich domain in the copolymer, hence, poor in HV units. Consistent with the obtained results, the melting temperatures of PHB and PHV are reported to be approximately  $179\text{ }^\circ\text{C}$  and between  $107$  and  $112\text{ }^\circ\text{C}$  [36], respectively. However, PHV melting temperature has not been clearly defined yet, in fact, Ishida et al. [52] reported very high HV content PHBV of narrow compositional distribution with melting temperatures of approximately  $100\text{ }^\circ\text{C}$ .

Apart from the presence of different copolymers in a blend, multiple melting peaks can be attributed to: (i) melting, recrystallization and remelting during heating; (ii) the presence of more than one crystal modification; (iii) different morphologies; (iv) physical aging; (v) different molecular weight species; and (vi) orientation effects, etc. [46].

A similar conclusion could be achieved by analyzing the trend of the Tg. It is possible to distinguish two values: one at about  $-11\text{ }^\circ\text{C}$ , corresponding to a more copolymeric domain, and another at about  $8\text{ }^\circ\text{C}$ , corresponding to the HB-rich domain. The presence of two Tg in almost all the cases confirmed the presence of different domains in the extracted PHAs batches.

Regarding the degree of crystallinity, by averaging the  $\chi$  across all the tested PHA,  $\chi$  is in the range of  $49\% \pm 8\%$ . These values are coherent with the crystallinity reported in the literature: crystallinities of around 60% for copolymers were observed by X-ray diffraction [37]. However, the minimum at the pseudoeutectic point is not visible.

It is important to highlight that this kind of estimation of crystallinity is affected by the perfection of the crystals formed. Indeed, Chen et al. [53] have shown that crystallinity obtained according to this method can be called the “equivalent weight crystallinity”, which means “the number of perfect crystals that can be melted by the measured enthalpy of melting”. The equivalent weight crystallinity does not only depend on the amount of

crystals, but also on the perfection of the crystals: a crystal with higher perfection has a larger equivalent weight.

The separated fractions obtained by the solvent/non-solvent extraction technique, as expected, showed a progressive increase in HV units. In fact, the lower the HV content, the less soluble the solution is, and, as a result, the fraction of polymers with the lowest content of HV units was the first to precipitate with the smallest addition of n-hexane, which was used as non-solvent. Fraction 1 of the fractionated PHA was obtained without adding n-hexane, indeed, it was not soluble in chloroform. As a result, this fraction could be characterized neither by  $^1\text{H-NMR}$  nor  $^{13}\text{C-NMR}$ . The insolubility in chloroform, coherently with the DSC outcomes, suggests that fraction 1 was constituted by HB units only (PHB), or with only trace amounts of HV. For the characterizable fractions, the HV content was 11 mol%, 35 mol%, 88 mol% for fraction 2, fraction 3 and fraction 4, respectively.

The results of thermal analysis on the fractions clearly show the presence of many domains with different relative compositions in terms of HV:HB in the extracted polymer. The absence of some of these intermediate peaks for the as-extracted PHAs in DSC scans could be explained considering that the complex mixture of random copolymers or block copolymers, could slow down or eventually suppress the crystallization of the domains with an intermediate content of HV units, having the slowest crystallization rates. In fact, the crystallization rate decreases by introducing HV units in PHB, showing its minimum when PHBV is at its pseudoeutectic composition (corresponding to HV content of about 50%) [37]. Consistent with this trend, in our study, the two extreme compositions (high HB and high HV content domains) always showed the ability to crystallize, either isolated or in the blend; while the intermediate compositions (around the pseudoeutectic) could not form crystalline structures in the blends, but only when isolated (Figure 7).

## 5. Conclusive Remarks

Co-fermentation of waste sludge microalgae mixed cultures grown of the liquid fraction of digestate was proven to be feasible. Sludge fermentation always produced a higher amount of VFAs than microalgae fermentation (with a maximum degree of acidification of 0.4 and 0.3 gCOD/gVS, respectively). The dominant short-chain fatty acid for all the tests was always acetate, followed by propionate.

PHAs produced by mixed VFAs, including microalgae as a source, proved to be a blend of different composition copolymers. In some cases, crystallinity was nearly completely suppressed, suggesting the potential employment of these polymers as flexible plastics or coating material.

The sustainability of these materials is two-fold: (i) it provides a bio-based alternative to synthetic plastics, (ii) it takes advantage of second-generation feedstocks, such as wastewaters and their treatment by-products, thus relieving the competition for first-generation feedstocks that are better suited for the feed and food market. By scaling up the process and by optimizing the extraction step, it will be possible to obtain reliable data for a proper life cycle analysis of the materials described in this paper.

**Author Contributions:** Conceptualization, S.T., E.F. and N.F.; validation, S.B. and R.C.; writing—original draft preparation, S.B.; writing—review and editing, R.C.; supervision, S.T. All authors have read and agreed to the published version of the manuscript.

**Funding:** This research was funded by CARIPLO FOUNDATION, grant number 2018-0992.

**Institutional Review Board Statement:** Not applicable.

**Informed Consent Statement:** Not applicable.

**Data Availability Statement:** The data presented in this study are available on request from the corresponding author. The data are not publicly available due to privacy.

**Conflicts of Interest:** The authors declare no conflict of interest.

## References

1. Single-Use Plastics. Available online: [http://ec.europa.eu/environment/waste/plastic\\_waste.htm](http://ec.europa.eu/environment/waste/plastic_waste.htm) (accessed on 25 January 2022).
2. Snell, K.D.; Peoples, O.P. PHA Bioplastic: A Value-Added Coproduct for Biomass Biorefineries. *Biofuels Bioprod. Biorefin.* **2009**, *3*, 456–467. [[CrossRef](#)]
3. Varsha, Y.M.; Savitha, R. Overview on Polyhydroxyalkanoates: A Promising Biopol. *J. Microb. Biochem. Technol.* **2011**, *3*, 99–105. [[CrossRef](#)]
4. Madkour, M.H.; Heinrich, D.; Alghamdi, M.A.; Shabbaj, I.I.; Steinbüchel, A. PHA Recovery from Biomass. *Biomacromolecules* **2013**, *14*, 2963–2972. [[CrossRef](#)] [[PubMed](#)]
5. Yu, J.; Chen, L.X.L. The Greenhouse Gas Emissions and Fossil Energy Requirement of Bioplastics from Cradle to Gate of a Biomass Refinery. *Environ. Sci. Technol.* **2008**, *42*, 6961–6966. [[CrossRef](#)]
6. Lu, J.; Tappel, R.C.; Nomura, C.T. Mini-Review: Biosynthesis of Poly(Hydroxyalkanoates). *Polym. Rev.* **2009**, *49*, 226–248. [[CrossRef](#)]
7. Boyandin, A.N.; Prudnikova, S.V.; Karpov, V.A.; Ivonin, V.N.; Đođ, N.L.; Nguyễn, T.H.; Lê, T.M.H.; Filichev, N.L.; Levin, A.L.; Filipenko, M.L.; et al. Microbial Degradation of Polyhydroxyalkanoates in Tropical Soils. *Int. Biodeterior. Biodegrad.* **2013**, *83*, 77–84. [[CrossRef](#)]
8. Reis, M.A.M.; Serafim, L.S.; Lemos, P.C.; Ramos, A.M.; Aguiar, F.R.; Van Loosdrecht, M.C.M. Production of Polyhydroxyalkanoates by Mixed Microbial Cultures. *Bioprocess Biosyst. Eng.* **2003**, *25*, 377–385. [[CrossRef](#)]
9. Serafim, L.S.; Lemos, P.C.; Oliveira, R.; Reis, M.A.M. Optimization of Polyhydroxybutyrate Production by Mixed Cultures Submitted to Aerobic Dynamic Feeding Conditions. *Biotechnol. Bioeng.* **2004**, *87*, 145–160. [[CrossRef](#)]
10. Chua, A.S.M.; Takabatake, H.; Satoh, H.; Mino, T. Production of Polyhydroxyalkanoates (PHA) by Activated Sludge Treating Municipal Wastewater: Effect of PH, Sludge Retention Time (SRT), and Acetate Concentration in Influent. *Water Res.* **2003**, *37*, 3602–3611. [[CrossRef](#)]
11. Villano, M.; Beccari, M.; Dionisi, D.; Lampis, S.; Micheli, A.; Vallini, G.; Majone, M. Effect of PH on the Production of Bacterial Polyhydroxyalkanoates by Mixed Cultures Enriched under Periodic Feeding. *Process. Biochem.* **2010**, *45*, 714–723. [[CrossRef](#)]
12. Dionisi, D.; Majone, M.; Vallini, G.; Di Gregorio, S.; Beccari, M. Effect of the Length of the Cycle on Biodegradable Polymer Production and Microbial Community Selection in a Sequencing Batch Reactor. *Biotechnol. Prog.* **2007**, *23*, 1064–1073. [[CrossRef](#)] [[PubMed](#)]
13. Frison, N.; Andreolli, M.; Botturi, A.; Lampis, S.; Fatone, F. Effects of the Sludge Retention Time and Carbon Source on Polyhydroxyalkanoate-Storing Biomass Selection under Aerobic-Feast and Anoxic-Famine Conditions. *ACS Sustain. Chem. Eng.* **2021**, *9*, 9455–9464. [[CrossRef](#)] [[PubMed](#)]
14. Oshiki, M.; Satoh, H.; Mino, T.; Onuki, M. PHA-Accumulating Microorganisms in Full-Scale Wastewater Treatment Plants. *Water Sci. Technol.* **2008**, *58*, 13–20. [[CrossRef](#)] [[PubMed](#)]
15. Johnson, K.; Kleerebezem, R.; Loosdrecht, M.C.M.V. Influence of the C/N Ratio on the Performance of Polyhydroxybutyrate (PHB) Producing Sequencing Batch Reactors at Short SRTs. *Water Res.* **2010**, *44*, 2141–2152. [[CrossRef](#)]
16. Meesters, K.P.H.; Van Loosdrecht, M.C.M. *Production of Poly-3-Hydroxyalkanoates from Waste Streams*; Delft University of Technology: Delft, The Netherlands, 1998.
17. Yu, J.; Si, Y. A Dynamic Study and Modeling of the Formation of Polyhydroxyalkanoates Combined with Treatment of High Strength Wastewater. *Environ. Sci. Technol.* **2001**, *35*, 3584–3588. [[CrossRef](#)]
18. Delgadillo-Mirquez, L.; Lopes, F.; Taidi, B.; Pareau, D. Nitrogen and Phosphate Removal from Wastewater with a Mixed Microalgae and Bacteria Culture. *Biotechnol. Rep.* **2016**, *11*, 18–26. [[CrossRef](#)]
19. All-Gas. Available online: <http://www.all-gas.eu> (accessed on 25 January 2022).
20. Ficara, E.; Uslenghi, A.; Basilico, D.; Mezzanotte, V. Growth of Microalgal Biomass on Supernatant from Biosolid Dewatering. *Water Sci. Technol.* **2014**, *69*, 896. [[CrossRef](#)]
21. Ge, S.; Champagne, P. Nutrient Removal, Microalgal Biomass Growth, Harvesting and Lipid Yield in Response to Centrate Wastewater Loadings. *Water Res.* **2016**, *88*, 604–612. [[CrossRef](#)]
22. Ciapponi, R.; Caretto, A.; Turri, S. Milan Polymer Days. In Proceedings of the Valorisation of Algal Wastes from Water Depuration Process: Convenient Fillers for Polymeric Matrices, Milan, Italy, 14–16 February 2018.
23. Ación, F.G.; Gómez-Serrano, C.; Morales-Amaral, M.M.; Fernández-Sevilla, J.M.; Molina-Grima, E. Wastewater Treatment Using Microalgae: How Realistic a Contribution Might It Be to Significant Urban Wastewater Treatment? *Appl. Microbiol. Biotechnol.* **2016**, *100*, 9013–9022. [[CrossRef](#)]
24. Mahdy, A.; Mendez, L.; Ballesteros, M.; González-Fernández, C. Algalculture Integration in Conventional Wastewater Treatment Plants: Anaerobic Digestion Comparison of Primary and Secondary Sludge with Microalgae Biomass. *Bioresour. Technol.* **2015**, *184*, 236–244. [[CrossRef](#)]
25. Li, Y.; Hua, D.; Zhang, J.; Zhao, Y.; Xu, H.; Liang, X.; Zhang, X. Volatile Fatty Acids Distribution during Acidogenesis of Algal Residues with PH Control. *World J. Microbiol. Biotechnol.* **2013**, *29*, 1067–1073. [[CrossRef](#)] [[PubMed](#)]
26. Cho, H.U.; Kim, Y.M.; Choi, Y.N.; Kim, H.G.; Park, J.M. Influence of Temperature on Volatile Fatty Acid Production and Microbial Community Structure during Anaerobic Fermentation of Microalgae. *Bioresour. Technol.* **2015**, *191*, 475–480. [[CrossRef](#)] [[PubMed](#)]
27. Gruhn, M.; Frigon, J.C.; Guiot, S.R. Acidogenic Fermentation of *Scenedesmus* Sp.-AMDD: Comparison of Volatile Fatty Acids Yields between Mesophilic and Thermophilic Conditions. *Bioresour. Technol.* **2016**, *200*, 624–630. [[CrossRef](#)] [[PubMed](#)]

28. Marazzi, F.; Bellucci, M.; Rossi, S.; Fornaroli, R.; Ficara, E.; Mezzanotte, V. Outdoor Pilot Trial Integrating a Sidestream Microalgae Process for the Treatment of Centrate under Non Optimal Climate Conditions. *Algal Res.* **2019**, *39*, 101430. [[CrossRef](#)]
29. Mantovani, M.; Marazzi, F.; Fornaroli, R.; Bellucci, M.; Ficara, E.; Mezzanotte, V. Outdoor Pilot-Scale Raceway as a Microalgae-Bacteria Sidestream Treatment in a WWTP. *Sci. Total. Environ.* **2020**, *710*, 135583. [[CrossRef](#)]
30. Conca, V.; da Ros, C.; Valentino, F.; Eusebi, A.L.; Frison, N.; Fatone, F. Long-Term Validation of Polyhydroxyalkanoates Production Potential from the Sidestream of Municipal Wastewater Treatment Plant at Pilot Scale. *Chem. Eng. J.* **2020**, *390*, R713–R715. [[CrossRef](#)]
31. Valentino, F.; Moretto, G.; Lorini, L.; Bolzonella, D.; Pavan, P.; Majone, M. Pilot-Scale Polyhydroxyalkanoate Production from Combined Treatment of Organic Fraction of Municipal Solid Waste and Sewage Sludge. *Ind. Eng. Chem. Res.* **2019**, *58*, 12149–12158. [[CrossRef](#)]
32. Morgan-Sagastume, F.; Valentino, F.; Hjort, M.; Cirne, D.; Karabegovic, L.; Gerardin, F.; Johansson, P.; Karlsson, A.; Magnusson, P.; Alexandersson, T.; et al. Polyhydroxyalkanoate (PHA) Production from Sludge and Municipal Wastewater Treatment. *Water Sci. Technol.* **2014**, *69*, 177–184. [[CrossRef](#)]
33. Kamiya, N.; Yamamoto, Y.; Inoue, Y.; Chujo, R.; Doi, Y. Microstructure of Bacterially Synthesized Poly(3-Hydroxybutyrate-Co-3-Hydroxyvalerate). *Macromolecules* **1989**, *22*, 1676–1682. [[CrossRef](#)]
34. Fiorese, M.L.; Freitas, F.; Pais, J.; Ramos, A.M.; de Aragao, G.M.F.; Reis, M.A.M. Recovery of Polyhydroxybutyrate (PHB) from *Cupriavidus Necator* Biomass by Solvent Extraction with 1,2-Propylene Carbonate. *Eng. Life Sci.* **2009**, *9*, 454–461. [[CrossRef](#)]
35. Chen, G.-Q. Plastics Completely Synthesized by Bacteria: Polyhydroxyalkanoates. In *Plastics from Bacteria: Natural Functions and Applications*; Chen, G.G.-Q., Ed.; Springer: Berlin/Heidelberg, Germany, 2010; pp. 17–37. ISBN 978-3-642-03287-5.
36. Laycock, B.; Arcos-Hernandez, M.V.; Langford, A.; Pratt, S.; Werker, A.; Halley, P.J.; Lant, P.A. Crystallisation and Fractionation of Selected Polyhydroxyalkanoates Produced from Mixed Cultures. *New Biotechnol.* **2014**, *31*, 345–356. [[CrossRef](#)] [[PubMed](#)]
37. Laycock, B.; Halley, P.; Pratt, S.; Werker, A.; Lant, P. The Chemomechanical Properties of Microbial Polyhydroxyalkanoates. *Prog. Polym. Sci.* **2014**, *39*, 397–442. [[CrossRef](#)]
38. Sialve, B.; Bernet, N.; Bernard, O. Anaerobic Digestion of Microalgae as a Necessary Step to Make Microalgal Biodiesel Sustainable. *Biotechnol. Adv.* **2009**, *27*, 409–416. [[CrossRef](#)] [[PubMed](#)]
39. Roberts, K.P.; Heaven, S.; Banks, C.J. Comparative Testing of Energy Yields from Micro-Algal Biomass Cultures Processed via Anaerobic Digestion. *Renew. Energy* **2016**, *87*, 744–753. [[CrossRef](#)]
40. Atasoy, M.; Owusu-Agyeman, I.; Plaza, E.; Cetecioglu, Z. Bio-Based Volatile Fatty Acid Production and Recovery from Waste Streams: Current Status and Future Challenges. *Bioresour. Technol.* **2018**, *268*, 773–786. [[CrossRef](#)] [[PubMed](#)]
41. Shen, L.; Hu, H.; Ji, H.; Cai, J.; He, N.; Li, Q.; Wang, Y. Production of Poly(Hydroxybutyrate-Hydroxyvalerate) from Waste Organics by the Two-Stage Process: Focus on the Intermediate Volatile Fatty Acids. *Bioresour. Technol.* **2014**, *166*, 194–200. [[CrossRef](#)]
42. Agler, M.T.; Wrenn, B.A.; Zinder, S.H.; Angenent, L.T. Waste to Bioproduct Conversion with Undefined Mixed Cultures: The Carboxylate Platform. *Trends Biotechnol.* **2011**, *29*, 70–78. [[CrossRef](#)]
43. Johnson, K.; Kleerebezem, R.; van Loosdrecht, M.C.M. Influence of Ammonium on the Accumulation of Polyhydroxybutyrate (PHB) in Aerobic Open Mixed Cultures. *J. Biotechnol.* **2010**, *147*, 73–79. [[CrossRef](#)]
44. Lemos, P.C.; Serafim, L.S.; Reis, M.A.M. Synthesis of Polyhydroxyalkanoates from Different Short-Chain Fatty Acids by Mixed Cultures Submitted to Aerobic Dynamic Feeding. *J. Biotechnol.* **2006**, *122*, 226–238. [[CrossRef](#)]
45. Takabatake, H.; Satoh, H.; Mino, T.; Matsuo, T. Recovery of Biodegradable Plastics from Activated Sludge Process. *Water Sci. Technol.* **2000**, *42*, 351–356. [[CrossRef](#)]
46. Arcos-Hernández, M.V.; Laycock, B.; Donose, B.C.; Pratt, S.; Halley, P.; Al-Luaibi, S.; Werker, A.; Lant, P.A. Physicochemical and Mechanical Properties of Mixed Culture Polyhydroxyalkanoate (PHBV). *Eur. Polym. J.* **2013**, *49*, 904–913. [[CrossRef](#)]
47. Žagar, E.; Kržan, A.; Adamus, G.; Kowalczyk, M. Sequence Distribution in Microbial Poly(3-Hydroxybutyrate-Co-3-Hydroxyvalerate) Co-Polyesters Determined by NMR and MS. *Biomacromolecules* **2006**, *7*, 2210–2216. [[CrossRef](#)]
48. Albuquerque, M.G.E.; Carvalho, G.; Kragelund, C.; Silva, A.F.; Barreto Crespo, M.T.; Reis, M.A.M.; Nielsen, P.H. Link between Microbial Composition and Carbon Substrate-Uptake Preferences in a PHA-Storing Community. *ISME J.* **2013**, *7*, 1–12. [[CrossRef](#)] [[PubMed](#)]
49. Morgan-Sagastume, F.; Karlsson, A.; Johansson, P.; Pratt, S.; Boon, N.; Lant, P.; Werker, A. Production of Polyhydroxyalkanoates in Open, Mixed Cultures from a Waste Sludge Stream Containing High Levels of Soluble Organics, Nitrogen and Phosphorus. *Water Res.* **2010**, *44*, 5196–5211. [[CrossRef](#)]
50. Munir, S.; Jamil, N. Polyhydroxyalkanoate (PHA) Production in Open Mixed Cultures Using Waste Activated Sludge as Biomass. *Arch. Microbiol.* **2020**, *202*, 1907–1913. [[CrossRef](#)] [[PubMed](#)]
51. Arcos-Hernandez, M.V.; Laycock, B.; Pratt, S.; Donose, B.C.; Nikolič, M.A.L.; Luckman, P.; Werker, A.; Lant, P.A. Biodegradation in a Soil Environment of Activated Sludge Derived Polyhydroxyalkanoate (PHBV). *Polym. Degrad. Stab.* **2012**, *97*, 2301–2312. [[CrossRef](#)]
52. Ishida, K.; Asakawa, N.; Inoue, Y. Structure, Properties and Biodegradation of Some Bacterial Copoly(Hydroxyalkanoate)s. *Macromol. Symp.* **2005**, *224*, 47–58. [[CrossRef](#)]
53. Chen, H.L.; Hwang, J.C. Some Comments on the Degree of Crystallinity Defined by the Enthalpy of Melting. *Polymer* **1995**, *36*, 4355–4357. [[CrossRef](#)]